Mon. Not. R. Astron. Soc. (2009) doi:10.1111/j.1365-2966.2008.14119.x

Deep analyses of nulling in Arecibo pulsars reveal further periodic behaviour

Jeffrey L. Herfindal[1]⋆ and Joanna M. Rankin[2]⋆

[1]*Department of Physics, Auburn University, Auburn, AL 36849, USA*
[2]*Physics Department, University of Vermont, Burlington, VT 05405, USA*

Accepted 2008 October 21. Received 2008 October 3; in original form 2008 January 21

ABSTRACT

Numerous studies of conal pulsars, e.g. B1133+16, have revealed fluctuation features and a steady null fraction. Sensitive Arecibo observations provide an unprecedented ability to detect nulls and confirm previously found fluctuation features. By replacing each pulse with a scaled version of the average profile, we were able to quench all subpulse modulation, dubbed pulse-modulation quelling (PMQ). It was surprising to note that the low-frequency feature observed in the natural longitude resolved fluctuation spectra (LRF) persisted in the PMQ LRFs. It appears that we can conclude, then, that in the natural pulse sequence the nulls themselves reflect whatever underlying periodicity is responsible for the low-frequency feature. Conversely, the aggregate fluctuation power of the low-frequency feature changes little whether the pulse modulation is quelled or not, implying that the feature fluctuations are *produced* by the nulls!

Key words: miscellaneous – methods: data analysis – pulsars: general.

1 INTRODUCTION

The complex inner workings of the pulsar emission mechanism still remain something of a mystery four decades after their discovery. Pulsar emission is both difficult and fascinating, in part because of its prominent modulation phenomena – in particular the 'big three' effects of subpulse drifting, 'mode' changing, and the pulse 'nulling' that is the subject of this paper.

The nulling phenomenon has been very perplexing since first identified by Backer (1970) because the nulls affected all components, even interpulses, and were simultaneous at all frequencies. Nulls thus appeared to represent a temporary cessation of the pulsar emission process, but strangely 'memory' was observed across nulls in some cases (Page 1973). Null fractions (*NF*) were computed for many of the known pulsars, and found to range from less than 1 to 70 per cent or so; but some half the stars appear not to null at all. The first systematic study of such *NF* was made by Ritchings (1976), who found a correlation between the *NF* and a pulsar's spindown age τ. Ten years later, Rankin (1986) showed that while old pulsars null more than young ones, many old pulsars do not null at all.

Ever more dramatic cases of extreme nulling – that is, apparent episodes of activity and inactivity – have been discovered over the intervening two decades: e.g. those of B0826−34 last for hours (Durdin et al. 1979); B1944+17 nulls 70 per cent of the time (Deich et al. 1986) and B1931+24 seems to cycle semiperiodically on a time-scale of a few weeks (Kramer et al. 2006).

⋆E-mail: J.Herfindal@gmail.com (JLH); Joanna.Rankin@uvm.edu (JMR)

Evidence has steadily accrued over the last few years that the nulls in many pulsars are not random turn-offs: the subpulse 'memory' across nulls in B0809+74 closely associates them with the star's drift (van Leeuwen et al. 2002, 2003); evidence of sputtering emission during nulls has been identified in both B0818−13 (Janssen & van Leeuwen 2004) and B1237+25 (Srostlik & Rankin 2005); almost all the nulls occur in one mode in B2303+30 (Redman, Wright & Rankin 2005); in B0834+06 the nulls tend to occur on the weak phase of the star's alternate-pulse modulation cycle (Rankin & Wright 2007), and finally the nulls in J1819+1305 exhibit a strong 57-stellar-rotation-period cyclicity (Rankin & Wright 2008). These circumstances strongly suggest that nulls, in many cases, represent 'empty' sightline traverses through a regularly rotating 'carousel' subbeam system (e.g. Deshpande & Rankin 2001).

In a recent paper (Herfindal & Rankin 2007, hereafter Paper I), we identified evidence for periodic nulling in pulsar B1133+16, a pulsar which exhibits no regular subpulse modulation. The nulls could be distinguished with great certainty in this star, and we then applied the straightforward method of filling the non-null pulses with the appropriately scaled-down average profile. This pulse-modulation quelling (PMQ) technique then confirmed that star's low-frequency modulation feature was associated with its nulls. Here, the implication is that this star's nulls are produced by a relatively stable, but irregular and sparsely filled carousel-beam system whose rotation gives a rough periodicity to 'empty' sightline passes. Such an interpretation may also explain Bhat et al.'s (2007) result that B1133+16's null pulses are not strictly simultaneous at all frequencies. They found about a 5 per cent excess of nulls at

metre wavelengths, and this may result from the star's larger conal emission pattern here.

These various current results lend new importance to understanding pulsar nulling more fully. Carousel-related '*pseudo*-nulls' may occur widely and explain much, but in certain stars the evidence is also very strong that their nulls represent a cessation of their emission, so at least two different types of nulls are implied. PSR B1931+24 shows several indications of this latter phenomenon: (i) the observed pulsar rotation during the 'on' cycle slows down 50 per cent faster than when 'off' and (ii) the emission changes from an active 'on' state to an 'off' state quasi-periodically, with the 'off' states lasting five orders of magnitude longer than typical nulling periods (Kramer et al. 2006).

Nulling is also closely associated with mode changing (e.g. Wang, Manchester & Johnston 2007), and the recently discovered rotating-radio transients (RRATs) naturally raise questions about the nature of such pulsars' long dormancies between their sporadic powerful bursts (McLaughlin et al. 2006).

Here, we continue the analytical effort begun in Paper I – i.e., applying the PMQ method to a small population of pulsars with conal profiles in order to test its efficacy and interpret its results in a larger context. Our Arecibo observations and analysis methods are briefly discussed in Section 2 and our results for each pulsar in Section 3. In Section 4, we summarize and discuss the results overall.

2 OBSERVATIONS AND METHODS

All of the observations were carried out using the 305-m Arecibo Telescope in Puerto Rico. Observations were conducted in the *P* band at 327 MHz. They used the same correction methods and instrumental techniques as in Paper I. Table 1 gives the resolution, length and date of each observation. The analytical techniques used in this paper are the same as those used in Paper I, but a brief description of each technique is given.

The null histogram for the pulsar B2034+19 is shown in Fig. 1. The integrated-intensity distribution of the pulses (solid line) and that of the off-pulse region (dashed line) are plotted. The off-pulse noise is included for every pulse, but due to the large number of off-pulse $\langle I \rangle$ values near zero, their distribution is scaled according to the highest on-pulse bin.

In Fig. 1, note the strong presence of pulses with zero (or near zero) aggregate intensity. However, note that the distribution is continuous between the pulses and nulls, frustrating any possibility of delineating the two populations positively. The dotted line represents the optimal boundary between putative nulls and pulses for the PSR B2034+19; 44 per cent of the pulses fall below this threshold.

Longitude-resolved fluctuation (hereafter LRF) spectra of the total power (Stokes *I*) were computed for all of the observations in Table 1 using fast Fourier transforms (hereafter FFTs) of length 256.[1] Fig. 2 shows the LRF spectra for pulsar B2034+19 with the aggregate spectrum (the middle panel) showing a clear feature at 0.0176 cycles per period (hereafter c/P_1, where P_1 is that particular pulsar's rotation period). The inverse of that frequency gives a P_3 value of $57 \pm 6P_1$. The inverse of the feature frequency (P_3) represents the rotation-period interval between bright subpulses at a given longitude. For each particular pulsar, these are the values reported as their features in Table 2.

PMQ was performed on each observation by computing a binary series of nulls and pulses, particular to each pulse sequence. To

[1] Pulsars B2303+30 and J0540+32 both used FFTs of length 512.

Table 1. Observational parameters.

Pulsar	Date (yr/d/m)	Length (pulses)	Resolution (deg/sample)
B0045+33	2005/07/01	1085	0.30
B0301+19	2005/08/01	1729	0.19
B0525+21	2003/04/10	636	0.35
	2006/07/10	961[a]	0.35
J0540+32	2006/07/10	1145	0.48
B0751+32	2003/04/10	1248	0.35
	2006/07/10	2080	0.35
B0823+26	2003/04/10	3392	0.35
B0834+06	2003/05/10	3789	0.35
	2006/06/05	1920	0.35
B1237+25	2003/12/07	2340	0.35
	2003/13/07	5094	0.35
	2003/20/07	4542	0.35
	2005/08/01	5209	0.13
J1649+2533	2005/06/01	1044	0.36
	2006/12/02	2818	0.36
J1819+1305	2006/12/02	3394	0.51
B1831−00	2005/07/01	1151	0.71
B1839+09	2005/07/01	1573	0.48
B1848+12	2003/19/10	2074	0.15
	2006/19/08	1037	0.48
B1918+19	2006/12/02	3946	0.39
B2034+19	2005/07/01	1676	0.36
B2122+13	2005/08/01	1038	0.36
B2303+30	2003/07/10	1526	0.23
B2315+21	2003/07/10	622	0.35
	2005/07/01	2491	0.26

[a] The last 121 pulses of this observation were ignored due to notable interference.

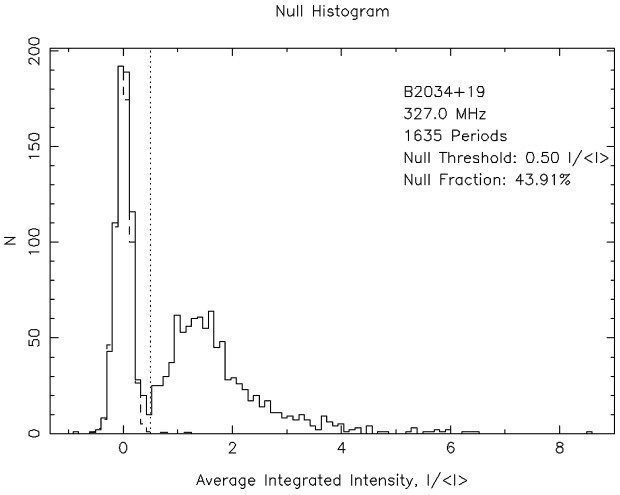

Figure 1. Null histogram for the pulsar B2034+19. The integrated-intensity distribution of the pulses (solid line) and that of the off-pulse region (dashed line) are plotted. The vertical dotted line represents an integrated-intensity threshold of $0.50\langle I \rangle$ to distinguish the nulls. Note that the null distribution is continuous with that of the pulses, frustrating any attempt to decisively measure the null fraction. Forty one (41) pulses were ignored due to bad baselines.

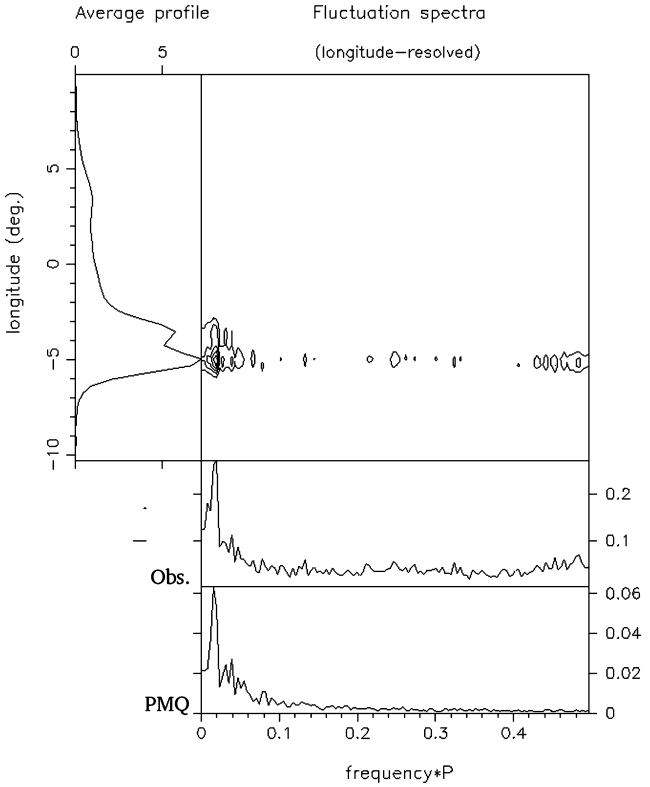

Figure 2. Typical LRF spectra for pulsar B2034+19 computed in total power (Stokes *I*). The main panel gives the spectra according to the average profile in the left-hand panel, and the integrated spectrum is shown in the middle panel. The LRF spectrum of the artificial 'PMQ' pulse sequence is given in the bottom panel. Most pulse modulation was quelled by substituting a scaled-down average profile for the pulses while zero intensity was substituted for putative nulls (see text). Here, as for most of the observations, an FFT length of 256 was used.

compute this, the null threshold from the pulse-intensity histogram was compared with the intensity of each pulse, within the same window, in order to determine if it was a pulse or putative null. An artificial pulse sequence was created corresponding to the natural one by substituting a scaled-down average profile for pulses and zero intensity for the 'null' pulses. The bottom panel of Fig. 2 shows the LRF spectrum of the PMQ pulse sequence for pulsar B2034+19. Note that the same low-frequency feature persists!

For the pulsars with multiple observations, the intensity values were combined in order to increase the sensitivity and to reduce the number of plots showing similar information. The null histograms were simply added together; whereas, for the LRF spectra (i.e. the integrated spectrum), in an effort to weight the observations appropriately, we used the observation length (number of pulses), this assuming that length was approximately proportional to total pulsar energy.

3 RESULTS FOR INDIVIDUAL PULSARS

B0301+19. This pulsar was found to have straight drift bands in both components on the pulse stack by Schönhardt & Sieber (1973). Weltevrede et al. (2006, 2007, hereafter W0607), using their two-dimensional Fourier analysis, found that the trailing component exhibits a broad drift feature with a larger P_3 value than in the leading one. The LRF spectrum in Fig. A2 (also those of W0607) shows two low-frequency features which correspond to much longer periodicities than any of the P_3 values reported. The $128 \pm 32P_1$ feature is prominent in the trailing component with the $51 \pm 5P_1$ feature appearing in both components. After PMQ analysis, only the 51-period feature remains. A null fraction around 10 per cent was reported earlier (Rankin 1986), our null histograms show a slightly larger value, on the order of 14 per cent.

B0525+21. Backer (1973) found that if emission occurs in component II then it can be predicted, reliably, that the next subpulses

Table 2. Observed low-frequency feature(s), features remaining after PMQ analysis, and null fractions (*NF*).

J2000 name	B1950 name	*NF* (per cent)	LRF Feature(s) (P_1)	PMQ Feature (P_1)	Figure
J0304+1932	B0301+19	14 ± 4	128 ± 32	–	A2
			51 ± 5	51 ± 5	
J0528+2200	B0525+21	28 ± 2	85 ± 14	85 ± 14	A3
			46 ± 4	46 ± 4	
J0540+32	–	54 ± 1	256 ± 64	256 ± 64	A4
J0754+3231	B0751+32	38 ± 6	64 ± 8	73 ± 10	A5
J0837+0610	B0834+06	9 ± 1	–	16 ± 4	A7
			2.17 ± 0.01	2.18 ± 0.01	
J1649+2533	–	25 ± 5	51 ± 5	64 ± 8	A9
			27 ± 2	27 ± 2	
			2.5 ± 0.2	–	
J1819+1305	–	41 ± 6	57 ± 6	64 ± 8	A10
J1841+0912	B1839+09	<2	37 ± 3	37 ± 3	A12
			28 ± 2	–	
J1921+1948	B1918+19	9 ± 2	85 ± 14	85 ± 14	A14
			–	43 ± 4	
J2037+1942	B2034+19	44 ± 4	57 ± 6	57 ± 6	Figs 1, 2, A15
J2305+3100	B2303+30	11 ± 2	102 ± 20	128 ± 32	A17
			–	64 ± 8	
			37 ± 3	37 ± 3	

will be in component I. He also found that the most prominent feature is at 0.025 c/P_1 (or 40P_1) and that it is present at all longitudes across the profile. Taylor, Manchester & Huguenin (1975) found a very weak preference for negative subpulse drift in adjacent pulses. Recently, W0607 found that the trailing component shows a positive drift at 21 cm, while there is evidence for a preferred negative drift direction in the leading component at 21 and 92 cm. Their spectra also show a welter of low-frequency features. Our LRF spectrum in Fig. A3 shows two bright, probably harmonically related features at 85±14 and 46 ± 4P_1, which survive the PMQ procedure almost unaltered. The null histograms show a continuous distribution of intensity between the pulses and putative nulls. The overall null fraction is consistent with Ritchings' (1976) value of 25 per cent.

J0540+32. This pulsar was among the first discovered by the Arecibo L-band Feed Array (ALFA) pulsar surveys at Arecibo (Cordes et al. 2006). Although its null and pulse distributions are well separated, the distribution in Fig. A4 shows a number of pulses with intermediate intensity, and 54 per cent fall below our null threshold. There is a distinct very low-frequency feature with a period of 256 ± 64P_1 that survives the PMQ process virtually intact, though its length is so long relative to the FFT length that its period is not well measured.

B0751+32. At 430 MHz, Backus (1981) identified a preference for negative drift in this pulsar. Recently, W0607 found that the leading and trailing components show low-frequency features at 60 ± 20 and 70 ± 10P_1, respectively. The LRF spectrum in Fig. A5 exhibits many weak features as well as one corresponding to a period of 64 ± 8P_1 that survives the PMQ analysis. The null fraction of 38 ± 6 per cent from the intensity histogram is consistent with Backus's (1981) result of 34 per cent.

B0834+06. Taylor, Jura & Huguenin (1969) found a strong response at 0.462 c/P_1 (2.16 P_1) that was confirmed by Slee & Mulhall (1970). Sutton et al. (1970) identified it as a drift feature, Backer (1973) and Taylor et al. (1975) found a preference for positive subpulse drift, and recently Asgekar & Deshpande (2005) and W0607 confirmed the drifting feature's P_3 value of 2.2P_1. Rankin & Wright (2007) showed the pulsar's nulls are not randomly distributed but occur in a partial and periodic manner. The LRFs of our observations in Fig. A7 show a strong feature corresponding to some 2.17P_1 which remains after PMQ analysis. An unexpected response was revealed by the PMQ analysis at about 16P_1 that may represent the carousel circulation time. A null fraction of 7.1 per cent was determined by Ritchings (1976) and Rankin & Wright (2007) found that no more then 9 per cent of the star's pulses are nulls. Our observations permit very accurately determined pulse-energy distributions that nonetheless exhibit no definite boundary between the pulses and the putative nulls.

J1649+2533. This pulsar was found to have a null fraction of 30 per cent by Lewandowski et al. (2004). Our observations indicate a slightly lower null fraction on order of 25 per cent. They also found a P_3 value of 2.2P_1. Both of our observations show this feature on the outer edges of the star's profile, with a distinct gap in the centre. Two prominent low-frequency features can be seen in the LRF spectrum of Fig. A9 – one corresponding to some 27-odd P_1 and the other to about twice this, and both survive the PMQ analysis almost intact.

J1819+1305. A bright LRF feature at 57 ± 6P_1 is seen across the full width of the profile in Fig. A10, and this periodicity remains fully as prominent after PMQ analysis. Rankin & Wright (2008) investigated this pulsar's 'periodic nulls' in some detail, and they concluded that the nulls are probably produced by a subbeam-carousel system that rotates through our sightline with this period. In this pulsar's intensity histogram, the pulse and putative null distributions overlap strongly, deterring any possibility of accurately measuring its fraction of 'null' pulses.

B1839+09. W0607 confirmed the result (at 21 and 92 cm) found earlier by Backus (1981) to the effect that there is no preference in drift direction for the subpulse modulation. The LRF for this observation in Fig. A12 shows a strong feature that corresponds to a period of 37 ± 3P_1, and it also remains after PMQ was performed. The null histogram shows very clearly that the distribution of pulse intensities trails off into the null distribution, resulting in a null fraction of no more than 2 per cent.

B1918+19. Three drifting modes as well as a disordered mode were identified by Hankins & Wolszczan (1987). The putative null and pulse distributions overlap strongly in the pulse-energy histogram, but a threshold at 0.2 $\langle I \rangle$ is well motivated, giving a 9 per cent population of putative nulls. The LRF in Fig. A14 shows a surprisingly narrow low-frequency feature at 85 ± 14P_1 that, together with an apparent harmonic persists after PMQ analysis. Interestingly, the 12-P_1 periodicity also appears to be 'null' related.

B2034+19. This poorly studied pulsar has a large null population, and the pulse-intensity histogram in Fig. 1 indicates that 0.5 $\langle I \rangle$ provides a plausible threshold. On this basis, some 44 per cent of its pulses are nulls. Again, its low-frequency LRF feature corresponding to 57±6P_1 is remarkably well defined and, if anything, becomes more so following the PMQ analysis. Redman (2005) found that the pulsar exhibits null-demarcated modes, one in which only the leading part of the profile is strongly illuminated and with a nearly even-odd modulation, and a second wherein the entire profile is active with a strong P_3 of about 3.5P_1 on the profile edges.

B2303+30. Redman et al. (2005) found two distinct modes in this pulsar with almost all of the nulls occurring in the weaker '*Q*' (quiescent) mode. Fig. A17 shows that 11 per cent of the star's pulses fall below the 0.1 $\langle I \rangle$ null threshold in the pulse-energy histogram. The LRF spectra shows a broad, nearly even-odd modulated feature corresponding to the star's bright '*B*' mode as well as a wide distribution of '*Q*'-mode fluctuations around 3P_1. It also shows two prominent low-frequency features: one at 102 ± 20P_1 with the other at 37 ± 3P_1. These features remain after PMQ analysis, and the former seems to bifurcate into a 128 ± 32 and a 64 ± 8P_1 response.

4 DISCUSSION

Our surprise in Paper I was that the PMQ analysis associated B1133+16's low-frequency feature so clearly with its *nulls*! In this larger effort, we are no longer surprised to find abundant evidence for null-related periodicities in this population of conal dominated pulsars. We do, however, find pulsars whose nulls show no obvious periodicity as well as cases where PMQ reveals several, probably harmonically related, periodicities.

While these PMQ results do not prove that the various pulsar's patterns of pulses and nulls are produced by subbeam carousels rotating through our sightline, the characteristics of the modulation are largely compatible with this interpretation.

Specifically, the PMQ analysis did not always identify a null periodicity. Table 3 lists seven pulsars which clearly have a null fraction but do not, except for the pulsars: B1237+25 and B1831−00, have a clear LRF feature (Figs A8 and A11). These seven pulsars tend to produce either very broad features or featureless ('random') PMQ LRF spectra (see Figs A1, A6, A13, A16 and A18).

These featureless PMQ results could arise because (i) the modulation associated with a pulsar's LRF feature is not due to nulling

Table 3. Observed null fractions of 'featureless' pulsars.

J2000 name	B1950 name	*NF* (per cent)	Figure
J0048+3412	B0045+33	21 ± 3	A1
J0826+2637	B0823+26	7 ± 2	A6
J1239+2453	B1237+25	6 ± 1	A8
J1834−0010	B1831−00	<2	A11
J1851+1259	B1848+12	51 ± 2	A13
J2124+1407	B2122+13	21 ± 6	A16
J2317+2149	B2315+21	2.3 ± 0.5	A18

– e.g. PSR B1237+25 was found to have core-active and absent submodes within its normal mode, which alternate quasi-periodically about every $60P_1$ (Srostlik & Rankin 2005)[2] or (ii) the pulsar has nulls that are completely random – and thus a continuous 'white' PMQ aggregate fluctuation spectrum. If the emission process is governed by a rotating carousel subbeam system, a featureless PMQ spectrum could result if the pulsar: (i) had a highly irregular carousel circulation rate; (ii) a beamlet configuration that was short-lived with respect to its carousel circulation time or (iii) a very slow carousel circulation rate, for which, our observations are not long enough to detect a periodic pattern.

The amplitudes (or fluctuation power) of the PMQ-spectral features are in all cases smaller than the corresponding LRF spectral features – and often by a factor of about the respective *NF*. This could be taken to mean that the fluctuations produced by the 'nulls' are only a fraction of the modulation power that the LRF feature represents, and in a strict sense this is so, because in using the PMQ method it is only a subset of pulses based on the *NF* that produces this modulation. It is likely, however, that in the natural pulse sequence, the feature is produced by a much larger population of weak pulses and nulls – essentially the entire pulse sequence. Much more, surely, remains to be learned here which is beyond the scope of this study.

In all cases, the pulse-energy distributions were continuous with those of the null distributions. This result is compatible with a weak sputtering of the emission processes or a rotating subbeam-carousel mechanism.

The periodic nulling results of this paper amplify the evidence reviewed above to the effect that many pulsar nulls are neither random nor do they represent 'turn-offs' of the pulsar's emission mechanism. Rather, they seem to represent 'empty' passes of our sight-line through the carousel-beam pattern. Other recent evidence (e.g. B1931+24), however, all but confirms absolutely that some pulsar nulls do represent a complete or almost complete cessation of the emission. The conclusion then can hardly be escaped that a distinction must be maintained between pulsar nulls and a void sight-line transverse through the carousel-beam pattern.

ACKNOWLEDGMENTS

Portions of this work were carried out with support from US National Science Foundation Grant AST 99-87654. Arecibo Observatory is operated by Cornell University under contract to the US NSF. This work used the NASA ADS system.

[2] Some observations used in our analyses are the same as those used by Srostlik & Rankin; therefore we know that the observations we analysed (at least for B1237+25) do have these alternating modes.

REFERENCES

Asgekar A., Deshpande A. A., MNRAS, 2005, 357, 1105
Backer D. C., 1970, Nat, 228, 42
Backer D. C., 1973, ApJ, 182, 245
Backus P. R., 1981, PhD thesis, The University of Massachusetts
Bhat N. D. R., Gupta Y., Kramer M., Karastergiou A., Lyne A. G., Johnston S., 2007, A&A, 462, 257
Cordes J. M. et al., 2006, ApJ, 637, 446
Deich W. T. S., Cordes J. M., Hankins T. H., Rankin J. M., 1986, ApJ, 300, 540
Deshpande A. A., Rankin J. M., 2001, MNRAS, 322, 438
Durdin J. M., Large M. I., Little A. G., Manchester R. N., Lyne A. G., Taylor J. H., 1979, MNRAS, 186, 39
Hankins T. H., Wolszczan A., 1987, ApJ, 318, 410
Herfindal J. L., Rankin J. M., 2007, MNRAS, 380, 430 (Paper I)
Janssen G. H., van Leeuwen A. G. J., 2004, A&A, 425, 255
Kramer M., Lyne A. G., OBrien J. T., Jordan C. A., Lorimer D. R., 2006, Sci, 312, 549
Lewandowski W., Wolszczan A., Feiler G., Konacki M., Sołtysiński T., 2004, ApJ, 600, 905
McLaughlin M. A. et al., 2006 Nat, 439, 817
Page C. G., 1973, MNRAS, 163, 29
Rankin J. M., 1986, ApJ, 301, 901
Rankin J. M., Wright G. A. E., 2007, MNRAS, 379, 507
Rankin J. M., Wright G. A. E., 2008, MNRAS, 385, 1923
Redman S. R., 2005, Honors Thesis, Univ. Vermont
Redman S. R., Wright G. A. E., Rankin J. M., 2005, MNRAS, 357, 859
Ritchings R. T., 1976, MNRAS, 176, 249
Schönhardt R. E., Sieber W., 1973, Astrophys. Lett., 14, 61
Slee O. B., Mulhall P. S., 1970, Proc. Astron. Soc. Aust., 1, 322
Srostlik Z., Rankin J. M., 2005, MNRAS, 362, 1121
Sutton J. M., Staelin D. H., Price R. M., Weimer R., 1970, ApJ, 159, 89
Taylor J. H., Jura M., Huguenin G. R., 1969, Nat, 223, 797
Taylor J. H., Manchester R. N., Huguenin G. R., 1975, ApJ, 195, 513
van Leeuwen A. G. J., Kouwenhoven M. L. A., Ramachandran R., Rankin J. M., Stappers B. W., 2002, A&A, 387, 169
van Leeuwen A. G. J., Stappers B. W., Ramachandran R., Rankin J. M., 2003, A&A, 399, 223
Wang N., Manchester R. N., Johnston S., 2007, MNRAS, 377, 1383
Weltevrede P., Edwards R. T., Stappers B., 2006, A&A, 445, 243 (W06)
Weltevrede P., Stappers B. W., Edwards R. T., 2007, A&A, 469, 607 (W07)

APPENDIX A: RESULTS FOR THE INDIVIDUAL PULSARS

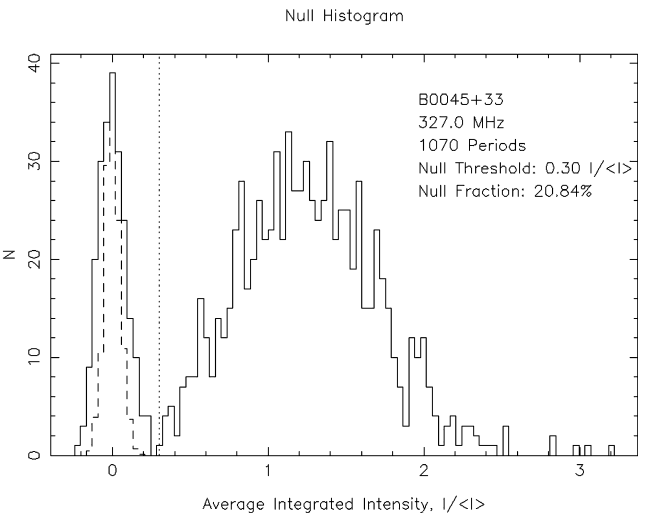

Figure A1. Null histogram for pulsar B0045+33 as in Fig. 2.

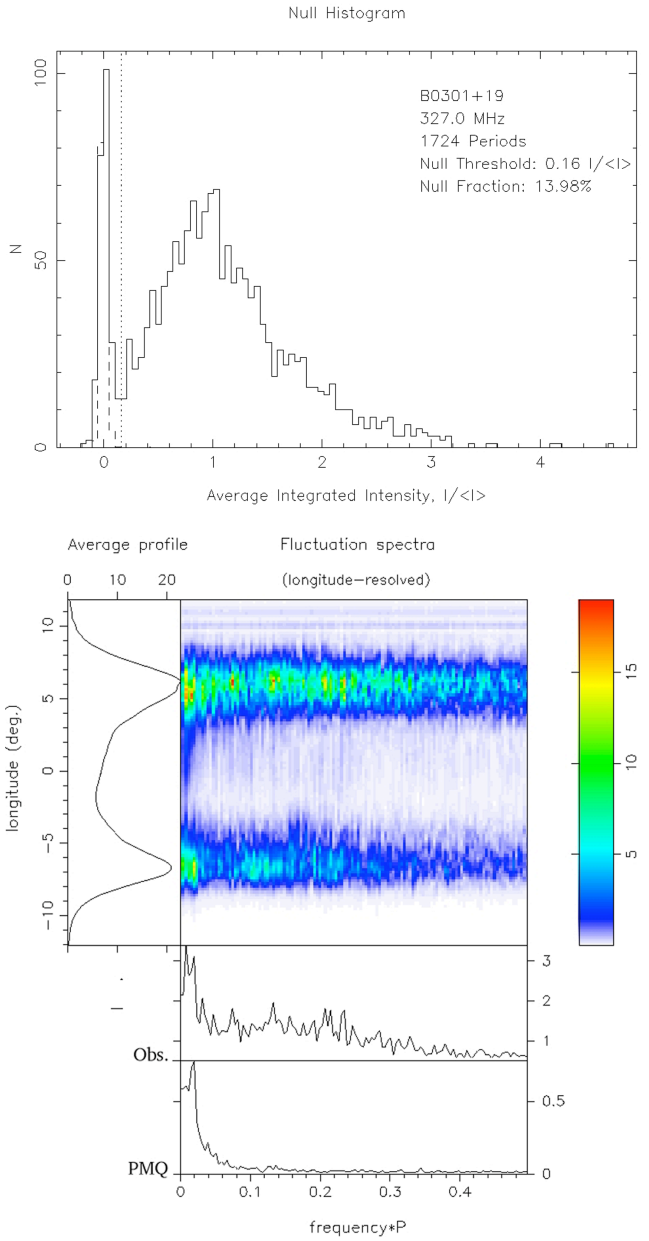

Figure A2. Null histogram (top, after Fig. 2) and LRF spectra (bottom, after Fig. 1) for pulsar B0301+19.

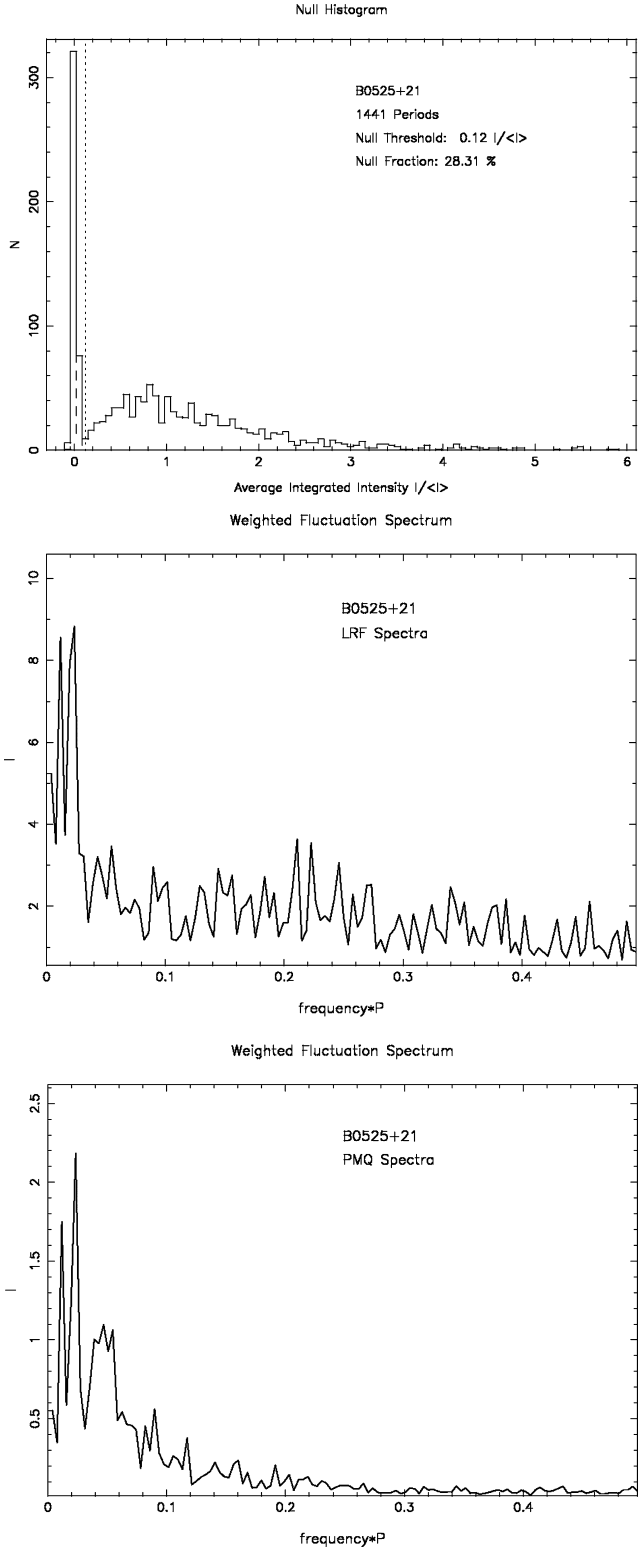

Figure A3. Null histogram (top, as in Fig. 2), LRF (middle) and PMQ (bottom) spectra for pulsar B0525+21. Here, several observations are combined in the three plots and the spectra weighted by the observation length (see text).

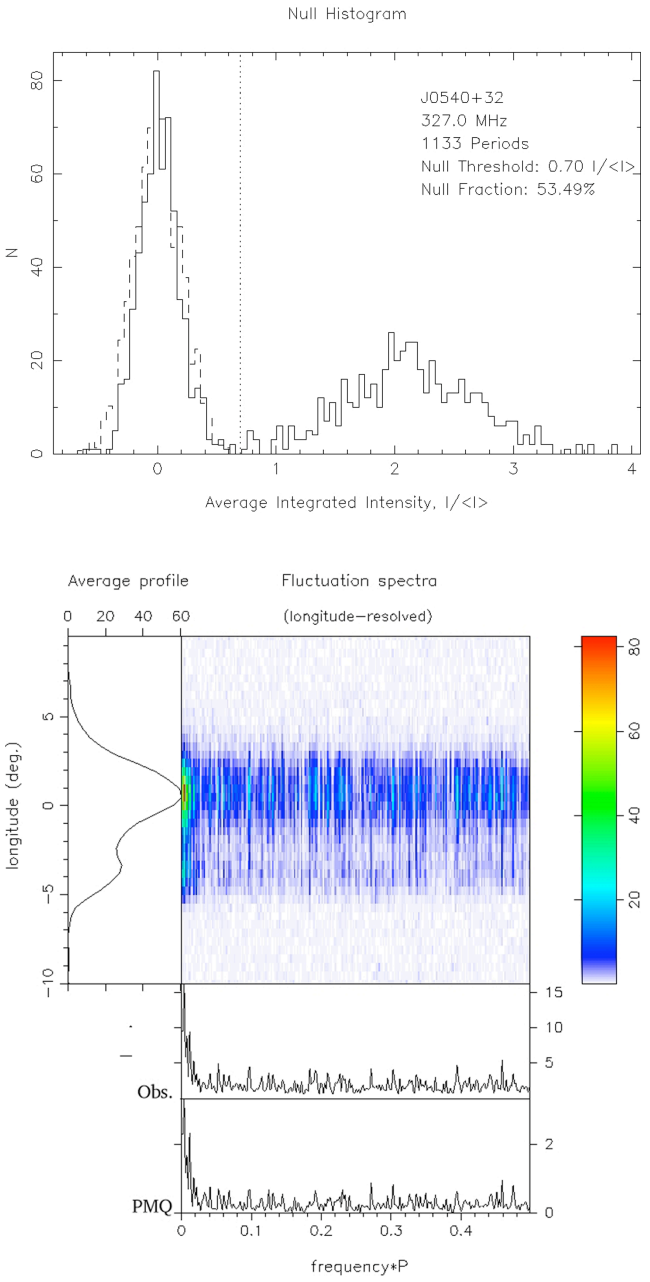

Figure A4. Null histogram (top) and LRF spectra (bottom) for pulsar J0540+32 as in Fig. A2.

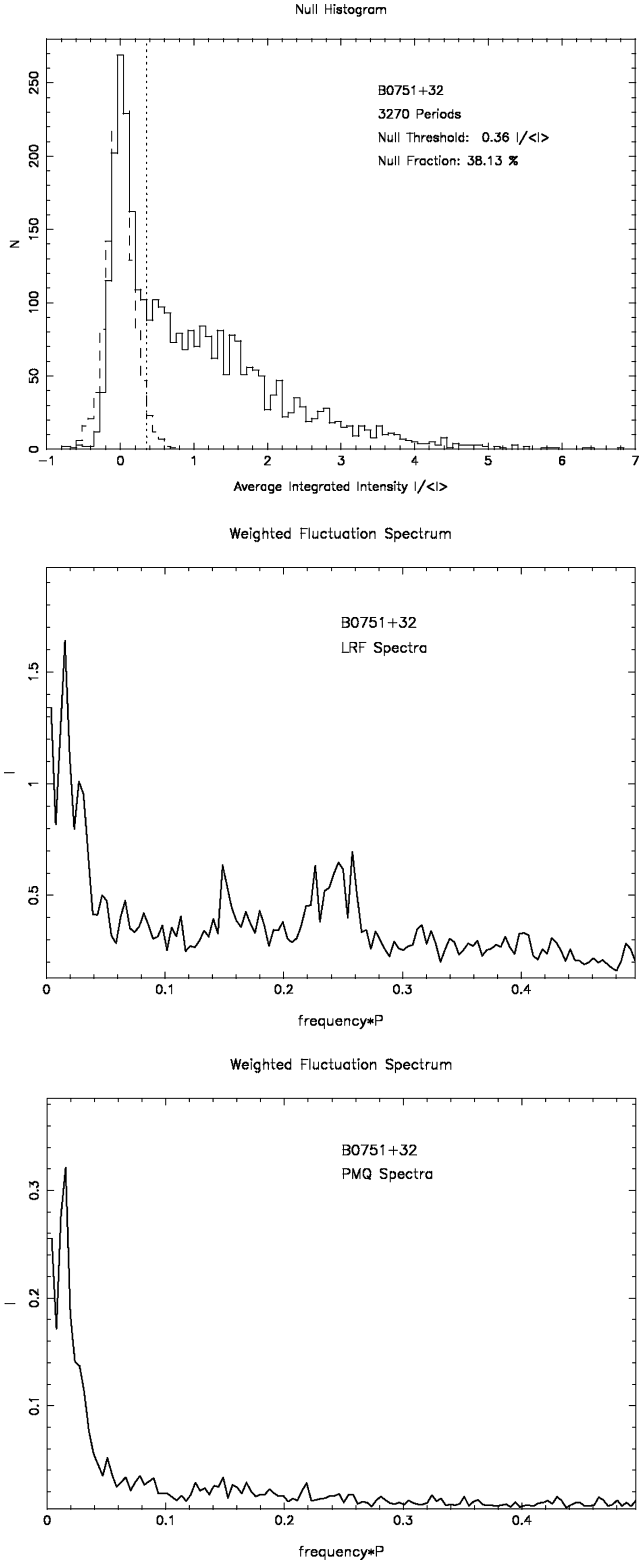

Figure A5. Null histogram (top), combined LRF (middle) and weighted PMQ (bottom) spectra for pulsar B0751+32 as in Fig. A3.

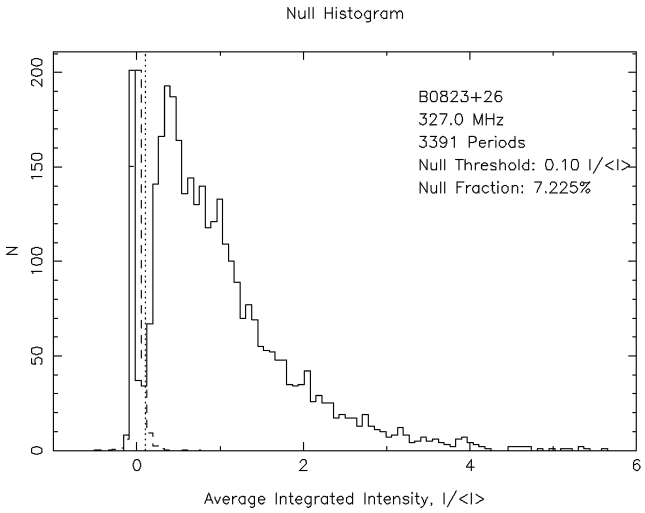

Figure A6. Null histogram for pulsar B0823+26, as in Fig. A1.

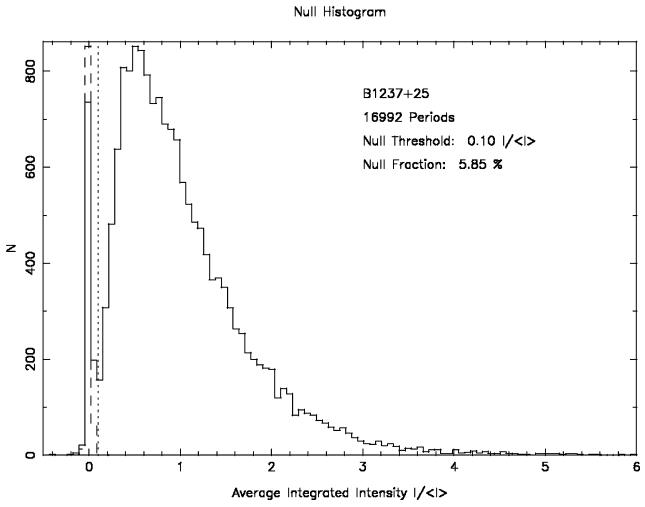

Figure A8. Combined null histogram for pulsar B1237+25, as in Fig. A3.

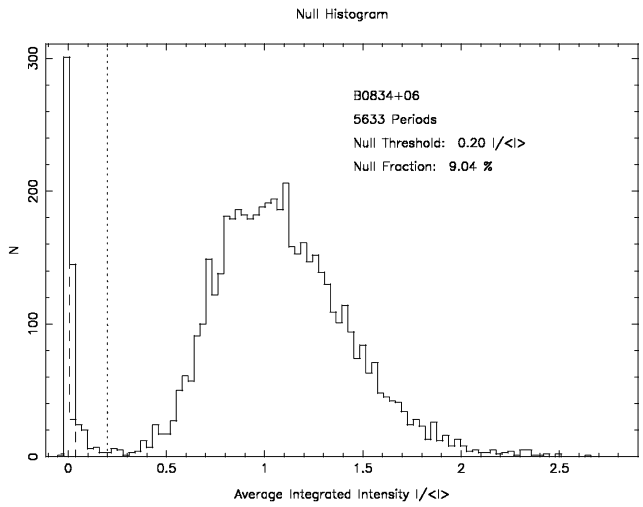

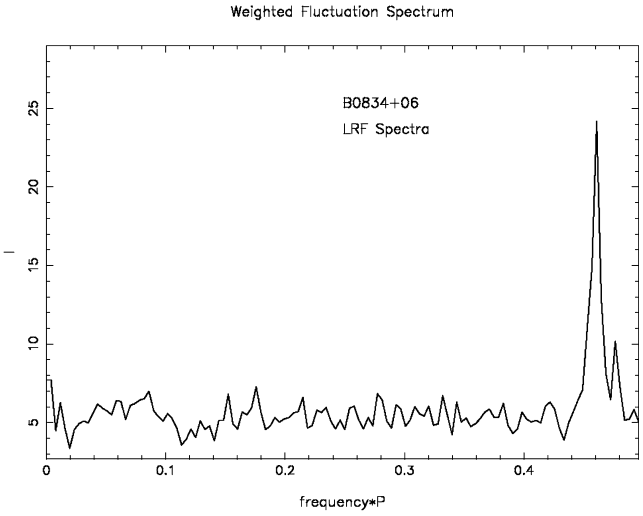

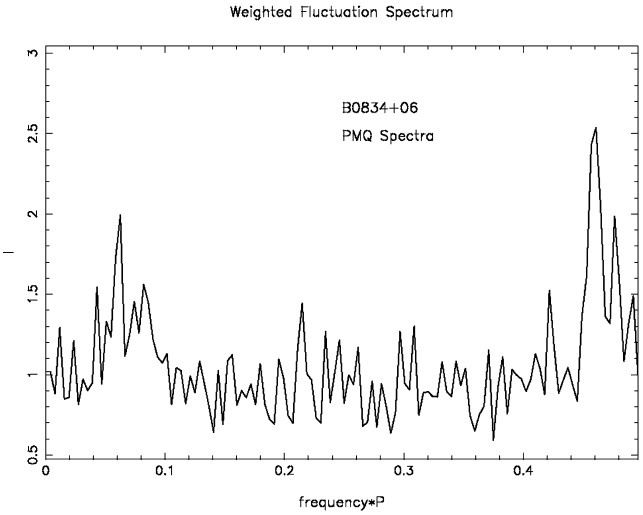

Figure A7. Null histogram (top), combined LRF (middle) and weighted PMQ (bottom) spectra for pulsar B0834+06 as in Fig. A3.

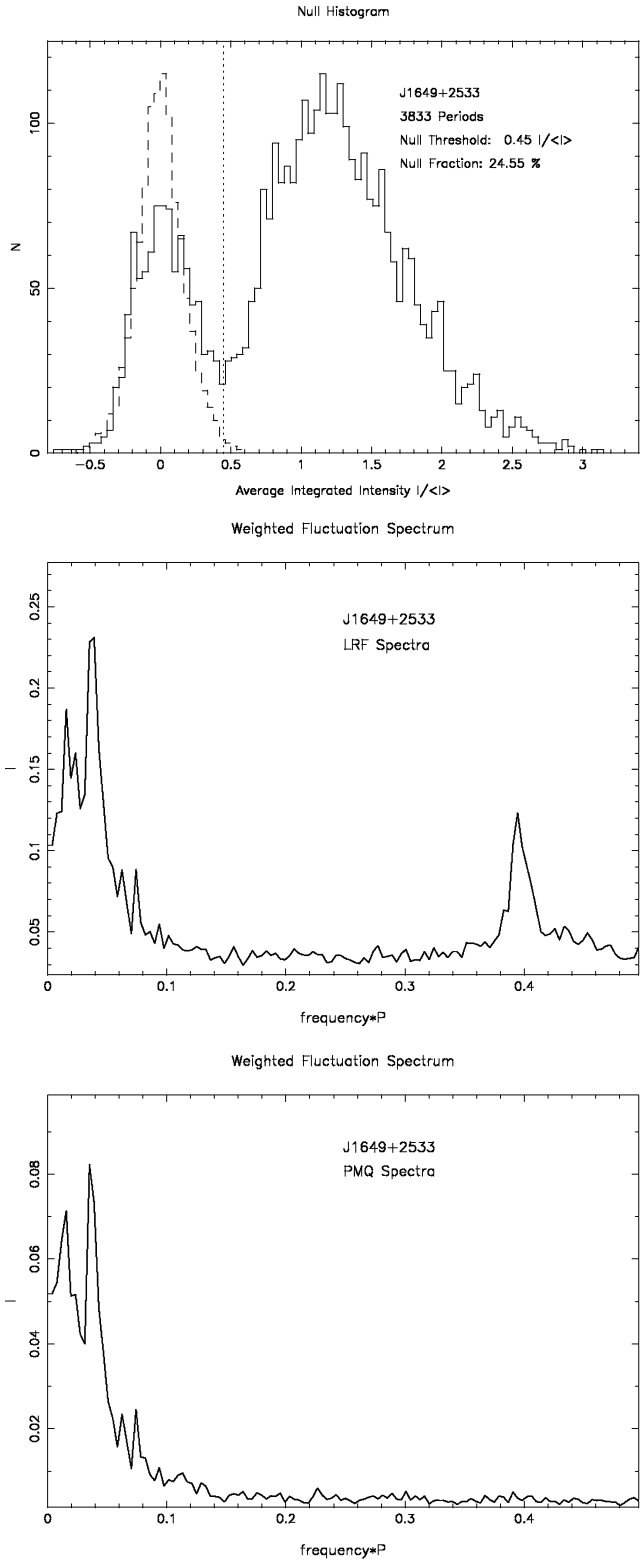

Figure A9. Null histogram (top), combined LRF (middle) and weighted PMQ (bottom) spectra for pulsar J1649+2533 as in Fig. A3.

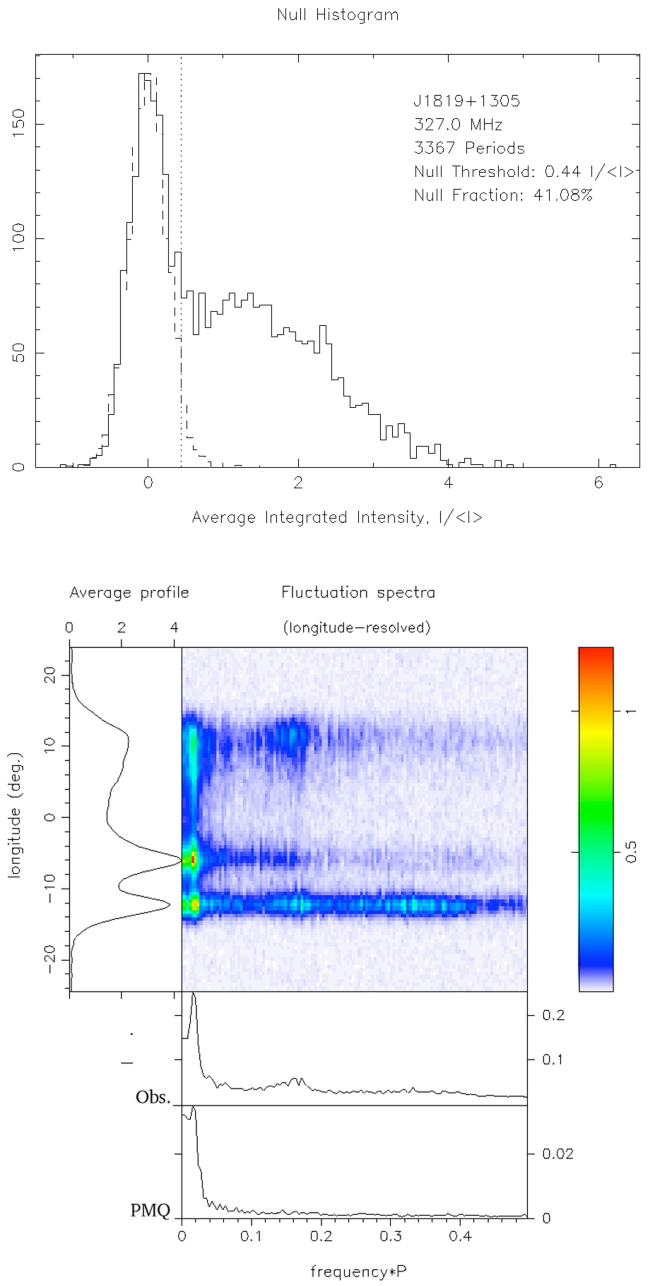

Figure A10. Null histogram (top) and LRF spectra (bottom) for pulsar J1819+1305 as in Fig. A2.

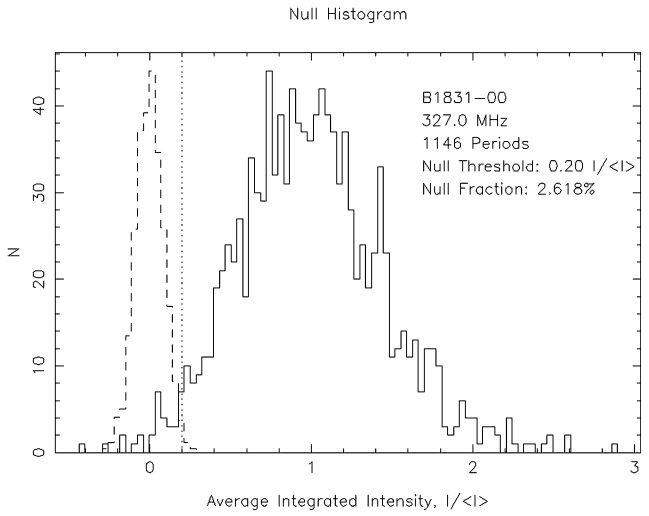

Figure A11. Null histogram (top) and LRF spectra (bottom) for pulsar B1831−00 as in Fig. A2.

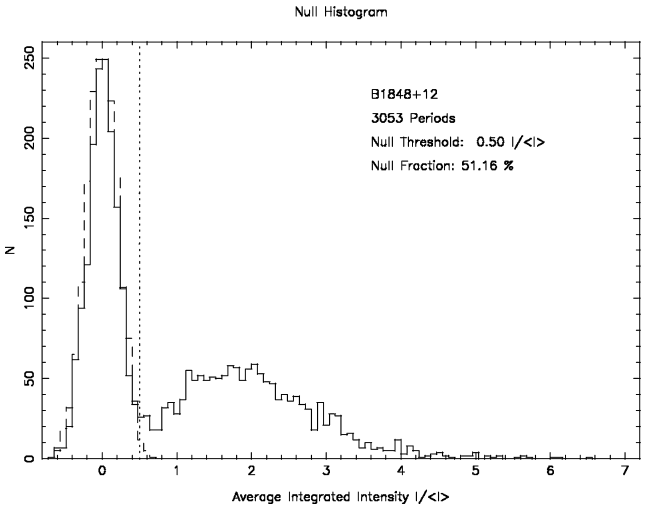

Figure A13. Combined null histogram for pulsar B1848+12, as in Fig. A3.

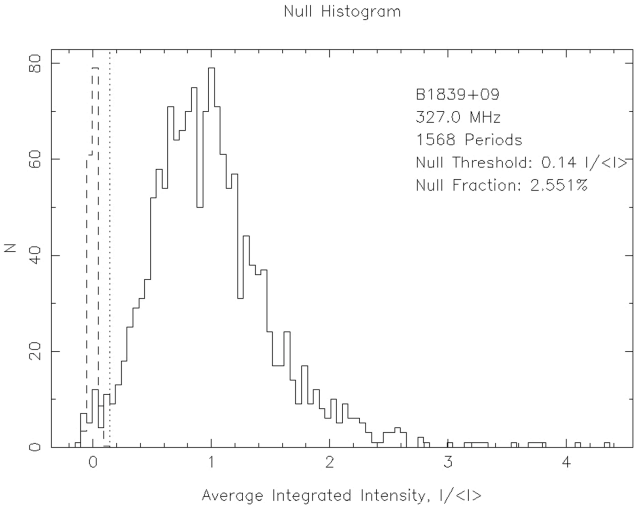

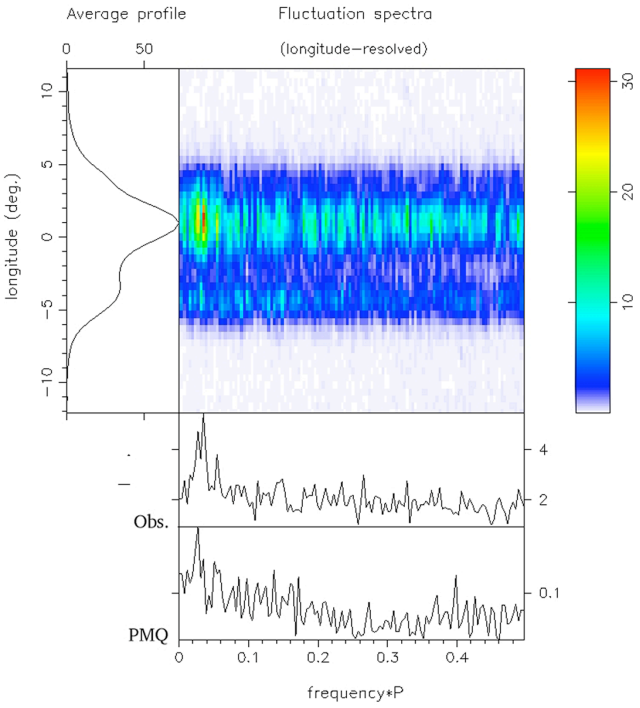

Figure A12. Null histogram (top) and LRF spectra (bottom) for pulsar B1839+09 as in Fig. A2.

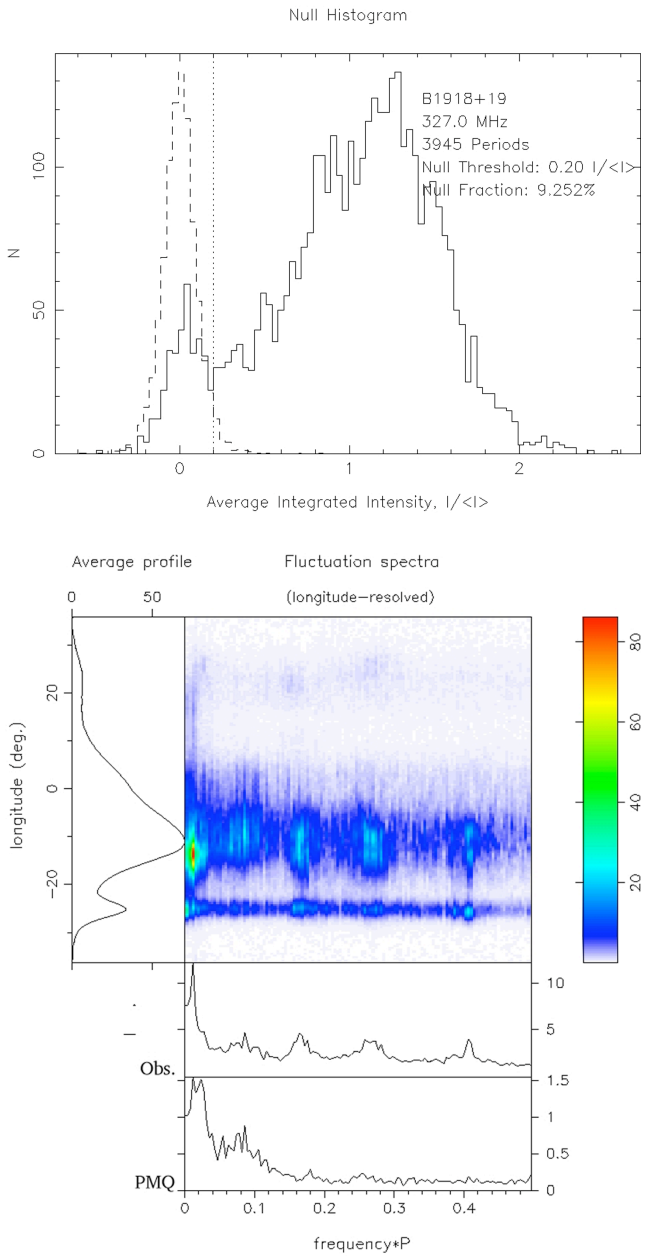

Figure A14. Null histogram (top) and LRF spectra (bottom) for pulsar B1918+19 as in Fig. A2.

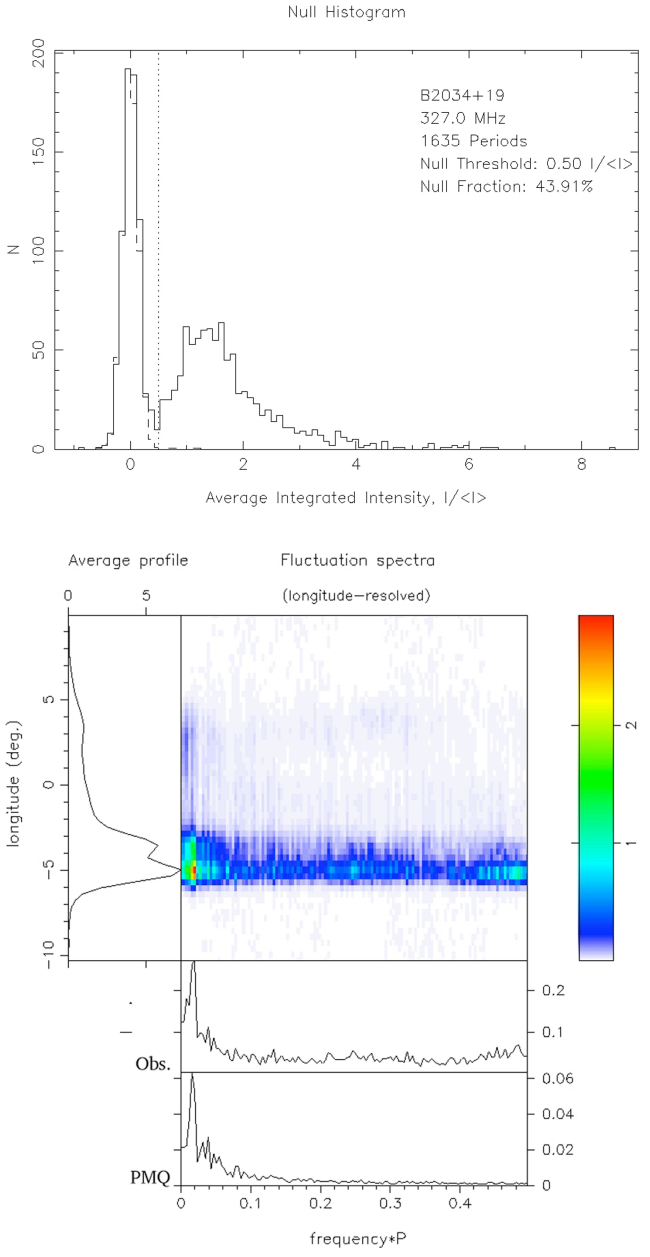

Figure A15. Null histogram (top) and LRF spectra (bottom) for pulsar B2034+19 as in Fig. A2.

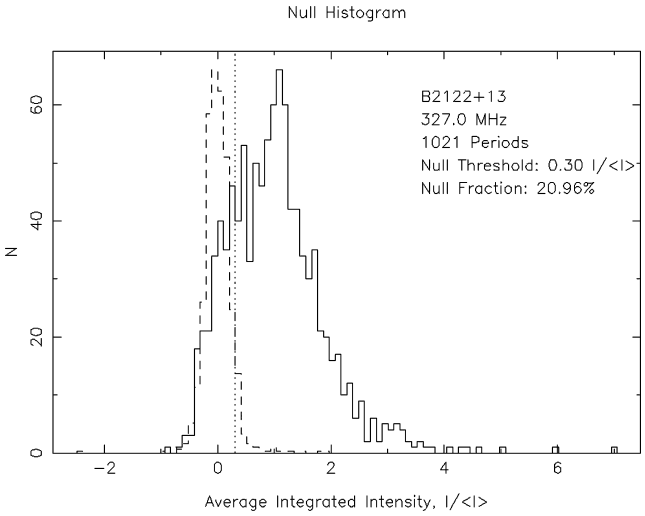

Figure A16. Null histogram for pulsar B2122+13, as in Fig. A1.

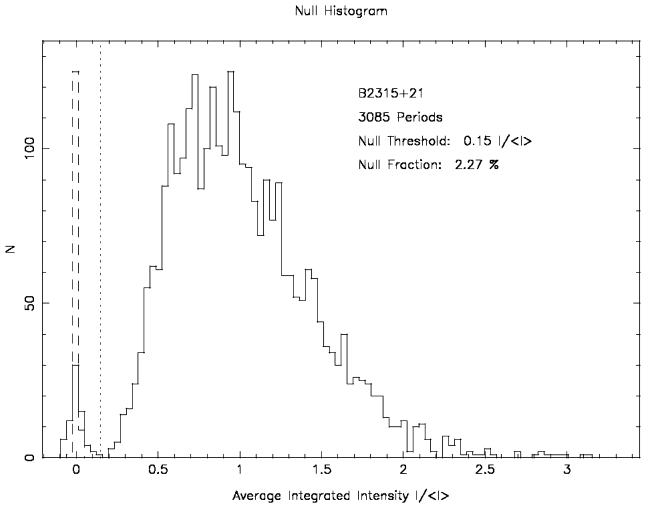

Figure A18. Null histogram for pulsar B2315+21, as in Fig. A1.

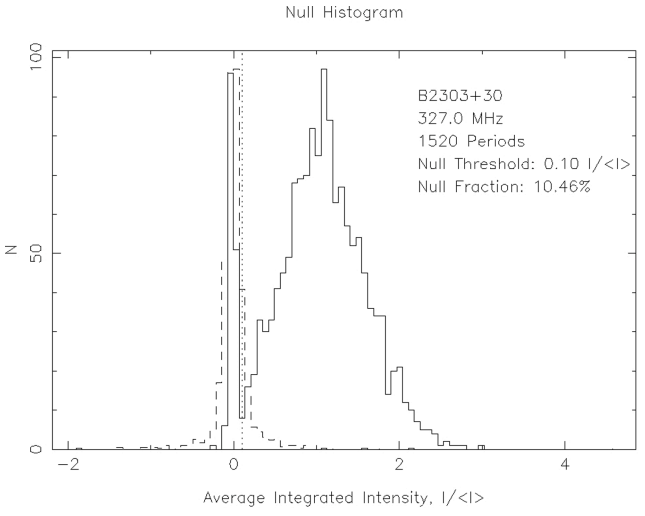

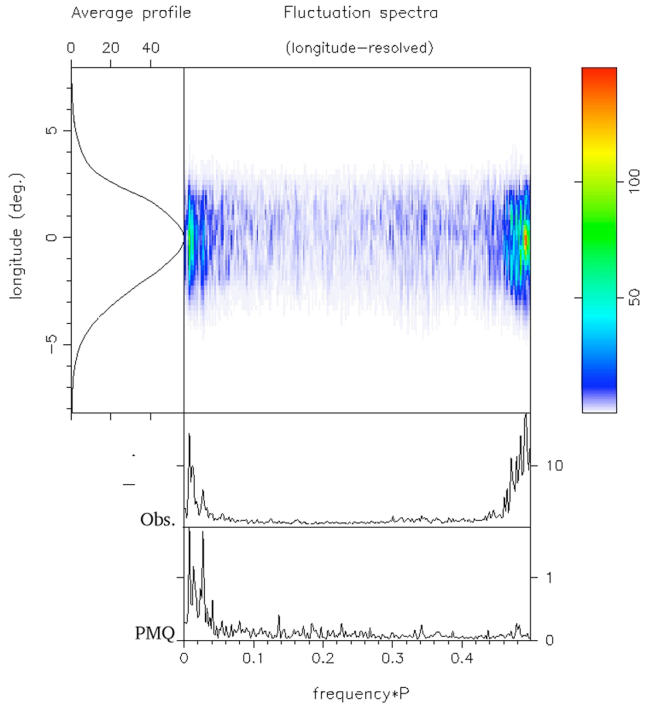

Figure A17. Null histogram (top) and LRF spectra (bottom) for pulsar B2303+30 as in Fig. A2.

This paper has been typeset from a TEX/LATEX file prepared by the author.